This article has been accepted for publication in a future issue of this journal, but has not been fully edited. Content may change prior to final publication. Citation information: DOI 10.1109/TBME.2015.2470641, IEEE Transactions on Biomedical Engineering

Noninvasive Estimation of Respiratory Mechanics in Spontaneously Breathing Ventilated Patients: A Constrained Optimization Approach

Francesco Vicario*, Antonio Albanese, Nikolaos Karamolegkos, Dong Wang, Adam Seiver, and Nicolas W. Chbat, *Members, IEEE*

***Abstract*— This paper presents a method for breath-by-breath noninvasive estimation of respiratory resistance and elastance in mechanically ventilated patients. For passive patients, well-established approaches exist. However, when patients are breathing spontaneously, taking into account the diaphragmatic effort in the estimation process is still an open challenge. Mechanical ventilators require maneuvers to obtain reliable estimates for respiratory mechanics parameters. Such maneuvers interfere with the desired ventilation pattern to be delivered to the patient. Alternatively, invasive procedures are needed. The method presented in this paper is a noninvasive way requiring only measurements of airway pressure and flow that are routinely available for ventilated patients. It is based on a first-order single-compartment model of the respiratory system, from which a cost function is constructed as the sum of squared errors between model-based airway pressure predictions and actual measurements. Physiological considerations are translated into mathematical constraints that restrict the space of feasible solutions and make the resulting optimization problem strictly convex. Existing quadratic programming techniques are used to efficiently find the minimizing solution, which yields an estimate of the respiratory system resistance and elastance. The method is illustrated via numerical examples and experimental data from animal tests. Results show that taking into account the patient effort consistently improves the estimation of respiratory mechanics. The method is suitable for real-time patient monitoring, providing clinicians with noninvasive measurements that could be used for diagnosis and therapy optimization.**

***Index Terms*—Mechanical ventilation, noninvasive parameter estimation, optimization, patient monitoring, respiratory mechanics, respiratory resistance, respiratory compliance.**

I. Introduction

MEASUREMENTS of the mechanical properties of the respiratory system are of paramount importance to clinicians for the management of mechanically ventilated patients. Quantitative assessment of respiratory mechanics can aid the clinician to: *1)* diagnose the disease underlying respiratory failure; *2)* monitor the status and progression of the disease; *3)* measure the effects of treatments; *4)* tune the ventilator settings to the patient specific needs, and thus minimize the risk of ventilator-induced complications, such as ventilator-induced lung injury (VILI) [1], [2].

Respiratory system mechanics is typically described via two parameters, the resistance (R) and the elastance (E), which account for the tendency of the system to oppose air flow and to return to its original volume after being stretched, respectively. For ventilated patients, methods for the assessment of R and E from noninvasive measurements of airway pressure and flow exist but they all present limitations.

A well-established technique is the inspiratory hold maneuver, also called flow interrupter technique (FIT) [3] or end-inspiratory pause (EIP). This technique consists of rapidly occluding the circuit through which the patient is breathing under conditions of constant inspiratory flow, while measuring the pressure in the circuit behind the occluding valve. The technique is noninvasive, easy to perform and the majority of the modern commercial ventilators have software that automates this procedure and computes resistance and elastance values. However, the maneuver interferes with the normal operation of the ventilator. As a result, it is not suitable for continual monitoring of respiratory mechanics and patient status. This is a severe limitation, as in critically ill patients the mechanical properties of the respiratory systems can rapidly change. Moreover and very importantly, the measurements provided by this technique are reliable only if the patient is completely passive throughout the duration of the inspiratory hold.

An alternative to the inspiratory hold maneuver consists of using the least squares (LS) method to fit a suitable mathematical model of the respiratory system to the pressure and flow measurements obtained noninvasively at the patient's airway [4], [5]. In this context, the most widely used mathematical representation of the respiratory system is the first-order single-compartment model that describes the system as an elastic compartment, representing the lung, served by a single resistive pathway, representing the upper airways [6]. Its parameters, R and E, can be either assumed constant (linear model), or varying with flow and/or volume

Manuscript submitted April 13, 2015; revised July 19, 2015; accepted August 8, 2015.

*F. Vicario (e-mail: francesco.vicario@philips.com), A. Albanese, N. Karamolegkos, D. Wang, and N. W. Chbat are with Philips Research North America, Briarcliff Manor, NY, USA. N. Karamolegkos is also with Columbia University, NY, USA. A. Seiver is with Philips Healthcare, Andover, MA, and Sutter Health, Sacramento, CA, USA.

This article has been accepted for publication in a future issue of this journal, but has not been fully edited. Content may change prior to final publication. Citation information: DOI 10.1109/TBME.2015.2470641, IEEE Transactions on Biomedical Engineering

(nonlinear models) [7]. Typically, data from an entire respiratory cycle are used in batch LS algorithms to estimate the values of R and E, thus allowing for breath-by-breath monitoring of respiratory mechanics. Adaptive algorithms, based on the recursive least squares (RLS) formulation with forgetting factor [8], have also been proposed to avoid the need for data storage and to allow for tracking of respiratory mechanics variations that correlate with disease progression [9]-[11].

The LS method provides some advantages over the inspiratory hold maneuver as it does not interfere with the normal operation of the ventilator. However, and similarly to the inspiratory hold maneuver, the LS method provides accurate results only if the patient is fully passive. During spontaneous breathing the pressure generated by the respiratory muscles (P_{mus}) is no longer a negligible driving force and the theoretical basis for the application of the LS method becomes invalid unless P_{mus} is a known input quantity [5]. To obviate these limitations, the additional measurement of esophageal pressure (P_{es}), which serves as a surrogate for intrapleural pressure (P_{pl}), can be included and the LS method can then be applied to transpulmonary pressure ($P_{ao} - P_{es}$) rather than airway pressure (P_{ao}) data. Khirani *et al*. [12], for instance, have proposed the use of transpulmonary pressure measurements to provide on-line monitoring of respiratory mechanics in spontaneously breathing patients, via application of LS-based algorithms. However, in this case, the assessment of respiratory mechanics is only limited to the lungs and the airways. It does not include the contribution of the chest wall to the elastance. Most importantly, computation of transpulmonary pressure requires continuous measurements of P_{es}, hence the insertion of a balloon-tipped catheter into the patient esophagus, as well as expert operators for correct placement and inflation of the balloon. This procedure also requires special equipment and attention to avoid errors and artifacts [13]. The invasive nature of the technique makes it unattractive in clinical settings.

From the above discussion, it emerges that monitoring of respiratory mechanics in ventilated patients with inspiratory activity is yet to be achieved, especially noninvasively. Moreover, in critical care medicine the popularity of partially assisted mechanical ventilation modes (where the patient can actively inspire, e.g., pressure support ventilation, PSV) has recently increased. These modes, in fact, are believed to promote patient respiratory muscles activation and weaning, thus resulting in better outcomes and reduced hospitalization costs [14]-[16]. Hence, a simple and reliable noninvasive technique for the assessment of respiratory mechanics in mechanically ventilated patients with spontaneous inspiratory efforts is a clear unmet clinical need. In an attempt to answer this need, several methods have been developed in the past few years.

Younes *et al*. have proposed the use of end-inspiratory occlusions [17] and pulses [18] to measure respiratory system elastance and resistance, respectively. Similarly, Lopez-Navas *et al*. [19] have used short expiratory occlusions, executed regularly at every 3 to 7 consecutive breaths, to estimate R and E via an algorithm fitting the difference between data from occluded and undisturbed breaths. Even though the introduction of pulses and occlusions in these methods have been shown to be clinically tolerable from a patient perspective, both methods still require some sort of maneuvers and hence interfere with the normal operation of the ventilator.

Chiew *et al*. [20] have developed a method that provides estimation of a time-varying elastance parameter in spontaneously breathing patients, without requiring any specific maneuver. However, the elastance parameter estimated by this method includes the confounding effects of the respiratory muscles pressure exerted by the patient.

Other methods that analyze pressure and flow data in the frequency domain, based on the principles of the forced oscillation technique (FOT), have also been proposed in the literature [21], [22]. FOT-based methods require the use of external small-amplitude pressure oscillations superimposed on the normal breathing, and hence special software/hardware modifications to the ventilator architecture.

In the present paper, we present a new method for noninvasive breath-by-breath estimation of respiratory mechanics in *actively* breathing patients *without* interfering with the normal operation of the mechanical ventilator and without requiring P_{es} measurements. The method uses air pressure and flow measured at the patient airway opening and it is based on the traditional first-order single-compartment model discussed above. The novel aspect of the method presented lies in the introduction of a constrained optimization (CO) algorithm that takes into account the presence of P_{mus} to render the estimation of R and E reliable even in the presence of patient effort. Simulated data have been used to validate the mathematical foundation of the method. Furthermore, the method has been applied to real data from animal tests and the reported results show potential for its extension to humans.

The paper is structured as follows. First, we describe the problem highlighting the challenges of the estimation of resistance and elastance in the presence of patient inspiratory efforts. Then, we provide a detailed description of the algorithm and we show via numerical simulations its strengths and limitations. Subsequently, we show experimental results on pigs. Finally, the method is critically discussed and future work is outlined.

II. Problem Statement

The lungs are traditionally represented as an elastic compartment (balloon) served by a single resistive pathway (airways), as shown in Fig. 1a. However simplistic this model is, it is nevertheless representative of the real lung mechanics and accepted in the respiratory research community. In Fig. 1a, the pressure at the entrance of the resistive pathway corresponds to the airway opening pressure (P_{ao}), whereas the pressure inside the balloon is representative of the alveolar pressure (P_{al}). The balloon, in turn, is enclosed in the chest wall that is represented as an additional elastic compartment whose internal pressure corresponds to intrapleural pressure (P_{pl}). The system is subject to an external pressure (P_{mus})

This article has been accepted for publication in a future issue of this journal, but has not been fully edited. Content may change prior to final publication. Citation information: DOI 10.1109/TBME.2015.2470641, IEEE Transactions on Biomedical Engineering

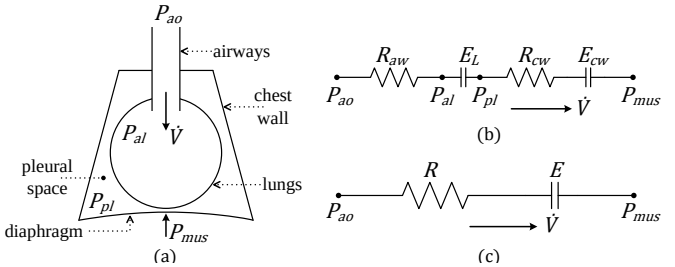

Fig. 1. (a) Schematic representation of respiratory mechanics; (b) electrical analogue; (c) lumped electrical analogue.

that represents an equivalent pressure of the force exerted by the respiratory muscles (mainly the diaphragm).

The electrical analogue corresponding to this schematic representation of the respiratory system is shown in Fig. 1b. The resistance and elastance elements of the airways/lungs are denoted as R_{aw} and E_L respectively, whereas the elastance of the chest wall is denoted as E_{cw}. An additional resistance R_{cw} is included to account for mechanical dissipation (friction) within the chest wall. The simplest model assumes that the resistive and elastic elements in the above electrical analogue are constant parameters.

The electrical analogue in Fig. 1b distinguishes between the airways/lungs and the chest wall components. For an equivalent and more compact representation of the model, the number of parameters can be reduced to two, namely the total resistance R and elastance E of the respiratory system (Fig. 1c). The air flow $\dot{V}(t)$ through the above mentioned elements is driven by the pressure difference $P_{ao}(t) - P_{mus}(t)$. In Fig. 1c, the equation governing respiratory mechanics, known as the equation of motion of the respiratory system, is

$$P_{ao}(t) = R\dot{V}(t) + EV(t) + P_{mus}(t) + P_0 \quad (1)$$

where $V(t)$ represents the volume of air inhaled from the beginning of inhalation ($t = 0$), and P_0 is a constant pressure term balancing the pressure at the airway opening at $t = 0$ ($V(0) = \dot{V}(0) = P_{mus}(0) = 0$).

Given (1) above, the problem at hand is to estimate the parameters R and E from measurements of $P_{ao}(t)$ and $\dot{V}(t)$ over one breath in spontaneously breathing mechanically ventilated patients. Note that the measurements of $V(t)$ can be obtained by numerical integration of $\dot{V}(t)$ over time, whereas P_0 and, most importantly, $P_{mus}(t)$ remain unknown.

Before plunging into the description of the method, it is useful to mention the main challenge of the above estimation problem and give an intuitive illustration. The problem is underdetermined, i.e., if we define R_{est}, E_{est}, $P_{est}(t)$ as possible estimates of R, E, $P_{mus}(t) + P_0$ in (1), there exist infinitely many solutions of triplets R_{est}, E_{est}, $P_{est}(t)$ satisfying (1) over a breath. Only one of them is *the* solution that we are after, i.e., R, E, $P_{mus}(t) + P_0$. To clarify this aspect, let us consider the electrical analogue in Fig. 1b and focus on airways and lung components only. The governing equation of motion can be written as

$$P_{ao}(t) = R_{aw}\dot{V}(t) + E_L V(t) + P_{pl}(t) + P_0' \quad (2)$$

where P_0' is, again, a constant pressure term to balance the equation at $t = 0$. Equation (2) is formally equivalent to (1). Hence, given the same set of measurements $P_{ao}(t)$, $\dot{V}(t)$ and $V(t)$, the set $R_{est} = R_{aw}$, $E_{est} = E_L$, $P_{est}(t) = P_{pl}(t) + P_0'$ satisfies (1) as well. As such, this would be another solution to the estimation problem we are considering. Moreover, many other solutions without physical interpretation exist. In fact, we could virtually choose any value for R_{est} and E_{est} and compute a corresponding estimated pressure profile $P_{est}(t)$ from

$$P_{est}(t) = P_{ao}(t) - R_{est}\dot{V}(t) - E_{est}V(t) \quad (3)$$

to find other solutions satisfying (1).

III. Method

The method we present is based on introducing constraints on the unknowns to be estimated, with the aim of overcoming the underdetermined nature of the mathematical problem. The constraints are based on physiology. For instance, the signal profile of the pressure exerted by the respiratory muscles does not change arbitrarily over one breath. It typically monotonically decreases at the beginning of a spontaneous breath, then monotonically increases when the muscles relax. In conditions of passive expiration, this pressure remains zero during exhalation. This physiological knowledge can then be infused in the estimation algorithm in the form of regional constraints where the monotonicity of $P_{mus}(t)$ is enforced via inequalities and equalities. For simplicity of mathematical formulation, in (1) we let $\tilde{P}_{mus}(t) = P_{mus}(t) + P_0$ as P_0 is constant over the breath. The estimation problem can then be cast as a constrained optimization problem with cost function

$$J = \sum_{k=1}^{k=N} \left(P_{ao}(t_k) - \left(R\dot{V}(t_k) + EV(t_k) + \tilde{P}_{mus}(t_k) \right) \right)^2 \quad (4)$$

to be minimized subject to the following constraints

$$\tilde{P}_{mus}(t_{k+1}) - \tilde{P}_{mus}(t_k) \leq 0 \quad \text{for } k = 1,2,\dots,m-1 \quad (5a)$$
$$\tilde{P}_{mus}(t_{k+1}) - \tilde{P}_{mus}(t_k) \geq 0 \quad \text{for } k = m, m+1, \dots, q-1 \quad (5b)$$
$$\tilde{P}_{mus}(t_{k+1}) - \tilde{P}_{mus}(t_k) = 0 \quad \text{for } k = q, q+1, \dots, N \quad (5c)$$

where t_k denotes the k[th] time sample, since the data are typically collected via sampling devices, and N is the total number of time samples in the breath. Defining the sampling time as Δt, then $t_1 = 0$, $t_2 = \Delta t$, ..., $t_k = (k-1)\Delta t$, ..., $t_N = (N-1)\Delta t$. The parameters t_m and t_q define the borders of the three regions of the breath in (5) with different monotonicity as illustrated in Fig. 2a. The cost function is of LS type, since the squared terms correspond to the difference between the measured P_{ao} and the one estimated from the model in (1) at each time sample. The unknowns over which J is minimized are R, E, $\tilde{P}_{mus}(t_1)$, …, $\tilde{P}_{mus}(t_N)$. Further constraints can be added on the range of values that $\tilde{P}_{mus}(t_k)$

This article has been accepted for publication in a future issue of this journal, but has not been fully edited. Content may change prior to final publication. Citation information: DOI 10.1109/TBME.2015.2470641, IEEE Transactions on Biomedical Engineering

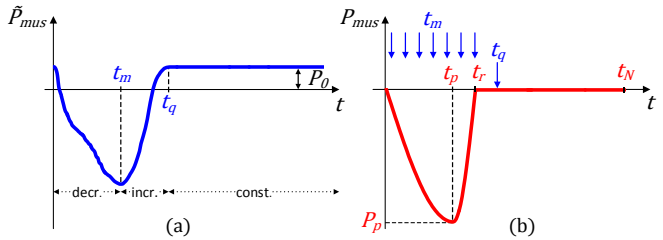

Fig. 2. (a) Regional constraints in (5) imposed on $\tilde{P}_{mus}(t)$ in the estimation method. The plot is an illustrative example of a possible profile satisfying such monotonicity constraints. (b) Nominal profile of $P_{mus}(t)$ used in the deterministic example. The profile is given by (11) with P_p=-5, t_p=0.45 and t_r=0.6. The constraints used in the estimation method are defined by t_q=0.8, whereas the search for the optimal t_m is done over the interval [t_1=0, t_r=0.6] in increments of 0.05.

can take and on the parameters R and E, which have to be positive, within some physiological bounds R_{max} and E_{max}

$$0 \le R \le R_{max} \tag{6a}$$
$$0 \le E \le E_{max} \tag{6b}$$
$$\tilde{P}_{min} \le \tilde{P}_{mus}(k) \le \tilde{P}_{max}. \tag{6c}$$

The constrained optimization problem in (4)-(6) is characterized by a quadratic cost function and linear constraints. It belongs to the class of so-called quadratic programs, which are a mature mathematical technique [23]. Well-established iterative algorithms such as the interior-point and active-set methods exist to solve this class of optimization problems and routines are available in most commercial software, e.g., Matlab®. To solve the minimization problem in (4)-(6) via such quadratic programming techniques, t_m and t_q in (5) need be specified. A search for the optimal t_m and t_q is then necessary. The search is done by solving the quadratic program for different pairs (t_m, t_q) and obtaining the corresponding minimized values J_{min}'s. The solution arising from the pair giving the minimum J_{min} among the obtained J_{min}'s provides the estimate of R and E. In practice, the possible candidates for (t_m, t_q) can be significantly reduced by exploiting information available from the ventilator. We narrow the search for t_m down to the interval $t_1 \le t_m < t_{SOE}$, whereas t_q can be fixed and equal to t_{SOE} (SOE stands for start of exhalation and denotes the time sample when the ventilator stops supporting the breath, a.k.a. cycling off). The rationale for this choice is that in normal conditions the ventilator cycles off when or after the patient effort terminates. More insight on the choice is given in the next section. To take advantage of available routines in commercial software, the quadratic program above is written in the standard form

$$\text{minimize} \quad J = \frac{1}{2}x^{\mathrm{T}}Hx + f^{\mathrm{T}}x + g \tag{7a}$$
$$\text{subject to} \quad Ax \le b \tag{7b}$$
$$A_{eq}x = b_{eq} \tag{7c}$$
$$l \le x \le u \tag{7d}$$

where

$$H = 2\begin{bmatrix} \sum_{k=1}^{N}\dot{V}^2(t_k) & \sum_{k=1}^{N}\dot{V}(t_k)V(t_k) & \dot{V}(t_1) & \dot{V}(t_2) & \cdots & \dot{V}(t_N) \\ \sum_{k=1}^{N}\dot{V}(t_k)V(t_k) & \sum_{k=1}^{N}V^2(t_k) & V(t_1) & V(t_2) & \cdots & V(t_N) \\ \dot{V}(t_1) & V(t_1) & 1 & 0 & \cdots & 0 \\ \dot{V}(t_2) & V(t_2) & 0 & 1 & \ddots & \vdots \\ \vdots & \vdots & \vdots & \ddots & \ddots & 0 \\ \dot{V}(t_N) & V(t_N) & 0 & \cdots & 0 & 1 \end{bmatrix} \tag{8a}$$

$$f^T = -2\begin{bmatrix} \sum_{k=1}^{N}\dot{V}(t_k)P_{ao}(t_k) & \sum_{k=1}^{N}V(t_k)P_{ao}(t_k) & P_{ao}(t_1) & \cdots & P_{ao}(t_N) \end{bmatrix} \tag{8b}$$

$$g = \sum_{k=1}^{N}P_{ao}^2(t_k), \quad l = \begin{bmatrix} 0 \\ 0 \\ \tilde{P}_{min} \\ \tilde{P}_{min} \\ \vdots \\ \tilde{P}_{min} \end{bmatrix}, \quad u = \begin{bmatrix} R_{max} \\ E_{max} \\ \tilde{P}_{max} \\ \tilde{P}_{max} \\ \vdots \\ \tilde{P}_{max} \end{bmatrix}, \quad b = 0, \quad b_{eq} = 0 \tag{8c}$$

$$A = \begin{bmatrix} 0 & 0 & -1 & 1 & 0 & \cdots & 0 & 0 & 0 & \cdots & 0 & 0 & 0 & \cdots & 0 \\ \vdots & \ddots & \ddots & \ddots & \ddots & & & & & & & & & & \vdots \\ & & & & \ddots & \ddots & \ddots & & & & & & & & \\ & & & & & -1 & 1 & 0 & & & & & & & \\ & & & & & & 1 & -1 & 0 & & & & & & \\ & & & & & & & \ddots & \ddots & \ddots & & & & & \\ & & & & & & & & \ddots & \ddots & \ddots & & & & \\ & & & & & & & & & \ddots & \ddots & \ddots & \ddots & & \vdots \\ 0 & \cdots & & & & & & & & & \cdots & 0 & 1 & -1 & 0 & \cdots & 0 \end{bmatrix}, x = \begin{bmatrix} R \\ E \\ \tilde{P}_{mus}(t_1) \\ \tilde{P}_{mus}(t_2) \\ \vdots \\ \tilde{P}_{mus}(t_{m-1}) \\ \tilde{P}_{mus}(t_m) \\ \tilde{P}_{mus}(t_{m+1}) \\ \vdots \\ \tilde{P}_{mus}(t_{q-1}) \\ \tilde{P}_{mus}(t_q) \\ \tilde{P}_{mus}(t_{q+1}) \\ \vdots \\ \tilde{P}_{mus}(t_N) \end{bmatrix} \tag{8d}$$

$$A_{eq} = \begin{bmatrix} 0 & 0 & 0 & 0 & \cdots & 0 & 0 & 0 & \cdots & 0 & -1 & 1 & 0 & \cdots & \cdots & 0 \\ \vdots & & & & & & & & & & & \ddots & \ddots & \ddots & & \vdots \\ & & & & & & & & & & & & \ddots & \ddots & \ddots & 0 \\ 0 & \cdots & & & & & & & & & & & \cdots & 0 & -1 & 1 \end{bmatrix}. \tag{8e}$$

In the following examples, the function `quadprog` available in the optimization toolbox of Matlab® is used to solve the quadratic program in (7). Note that the matrix H of the quadratic term in the cost function J is positive-semidefinite as all its eigenvalues are non-negative. Since H is the second derivative of J with respect to x, J is convex. However, it is not strictly convex as two eigenvalues are equal to 0. The corresponding eigenvectors span the plane of solutions with same minimum cost. Hence, different linear combinations of these two eigenvectors give rise to the infinitely many solutions of the estimation problem at hand, as mentioned in the *Problem Statement* section. The physiological constraints introduced in the optimization problem aim to make such a plane of minimizing solutions infeasible, except for the point corresponding to the solution that we are after.

IV. Numerical Validation

To demonstrate the validity of the new estimation method, numerical simulations have been performed. The simulations were performed for the PSV ventilation mode, where the waveform for $P_{ao}(t)$ is dictated by the ventilator until the cycling off. In what follows is a simplified logic that was used in the study to model the PSV ventilation mode. When the patient starts the breath (P_{mus} changing from 0 to negative values), ideal triggering is assumed for simplicity and the

This article has been accepted for publication in a future issue of this journal, but has not been fully edited. Content may change prior to final publication. Citation information: DOI 10.1109/TBME.2015.2470641, IEEE Transactions on Biomedical Engineering

ventilator provides pressure at the airway opening of the patient. $P_{ao}(t)$ increases exponentially from an initial value ($PEEP$) and approaches asymptotically the nominal PSV value. The time constant of the exponential function is denoted as T_{rise}. $\dot{V}(t)$ and $V(t)$ are computed solving the ordinary differential equation (1). $\dot{V}(t)$ reaches a maximum value ($\dot{V}_{peak}$) and then decreases. Once it crosses a threshold given by $E_{cycle}\dot{V}_{peak}$ ($0 < E_{cycle} < 1$), the ventilator cycles off, i.e., the inhalation valve shuts down and the exhalation circuit opens. The time at which the ventilator cycles off is indicated by t_{SOE}. After t_{SOE}, the ventilator is modeled as maintaining an exhalation pressure equal to $PEEP$. $P_{ao}(t)$ is typically higher than $PEEP$ due to the internal resistance R_v of the ventilator and tubing. In summary, the measurements of $P_{ao}(t)$, $\dot{V}(t)$ and $V(t)$ are simulated via the following equations

$$P_{ao}(t) = PEEP + PSV(1 - \exp(-t/T_{rise})) \quad (9a)$$
$$P_{ao}(t) = R\dot{V}(t) + EV(t) + P_{mus}(t) + PEEP \quad (9b)$$

for $0 \le t < t_{SOE}$ and

$$0 = (R + R_v)\dot{V}(t) + EV(t) + P_{mus}(t) \quad (10a)$$
$$P_{ao}(t) = R_v\dot{V}(t) + PEEP \quad (10b)$$

for $t_{SOE} \le t \le t_N$, where t_N stands for the time at which the breath ends. For each simulation, we choose the ventilator settings ($PEEP$, PSV, T_{rise}, E_{cycle}) as well as R_v and the nominal values for the patient parameters (R, E) and respiratory muscles pressure ($P_{mus}(t)$). During inhalation, we solve the ordinary differential equation (9b) for $V(t)$ and $\dot{V}(t)$ with the forcing function $P_{ao}(t)$ given by (9a). During exhalation, we solve the ordinary differential equation (10a) for $V(t)$ and $\dot{V}(t)$ and then compute $P_{ao}(t)$ from (10b). Equation (9b) comes from (1) with $P_0 = PEEP$. Equations (10a) and (10b) come from the model in Fig. 3, modified from Fig. 1c by the introduction of the exhalation resistance R_v between the patient airway opening and the exhalation chamber in the ventilator. The $PEEP$ terms cancel out in (10a). The data coming from (9) and (10) are then sampled at 100 Hz ($\Delta t = 0.01$ s).

For brevity, the units will be often omitted in the rest of the paper. Time will always be reported in s (seconds), all the pressure values ($P_{ao}, P_{mus}, PEEP, PSV$) in cmH_2O, V in l (liter), $\dot{V}$ in l/s, R in $cmH_2O{\cdot}s/l$ and E in cmH_2O/l. These are the units commonly used in clinical practice.

A. Deterministic Example

The first example is meant to show how the constraints introduced in the previous section are capable of overcoming the underdetermined nature of the original estimation problem.

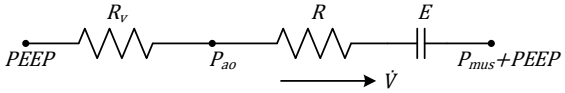

Fig. 3. Electrical analogue corresponding to (10).

Measurement noise is not taken into account here for clarity and will be discussed in the next section. Numerical experiments have revealed that the constraints introduced in the previous section are always able to make the solution of the quadratic program in (7) unique when the ventilator cycles off after the patient effort is over. For the purpose of illustration, we show here an example where the time at which the ventilator cycles off (t_{SOE}) is changed by varying the value of E_{cycle} over a broad range. The nominal profile of $P_{mus}(t)$ is chosen to be sinusoidal, as implemented for example in a commercial breathing lung simulator (ASL 5000, IngMar Medical). More precisely we simulate $P_{mus}(t)$ as

$$P_{mus}(t) = \begin{cases} P_p \sin\left(\frac{\pi}{2t_p}t\right) & \text{for } 0 \le t < t_p \\ P_p \sin\left(\frac{\pi}{2(t_r - t_p)}(t + t_r - 2t_p)\right) & \text{for } t_p \le t < t_r \\ 0 & \text{for } t_r \le t < t_N \end{cases} \quad (11)$$

where t_p and t_r indicate the time samples at which the nominal $P_{mus}(t)$ reaches its minimum (P_p, negative peak) and returns to 0, respectively. To better illustrate the key aspects of the method, in this example we exploit the knowledge of the nominal profile of $P_{mus}(t)$ to choose the estimation algorithm parameters t_m and t_q as follows: t_q is fixed as $t_q = t_r + 0.2$, whereas t_m varied between 0 and t_r ($t_1 \le t_m \le t_r$) in increments of 0.05. Fig. 2b graphically shows in the same plot the nominal profile of P_{mus} used to simulate P_{ao}, $\dot{V}$ and V waveforms and the algorithm constraint parameters t_m and t_q used in this example. Table I reports the estimation results from the measurements simulated for several values of E_{cycle}. As this parameter increases, the ventilator cycles off earlier. Note how the presented estimation method is able to find the nominal patient parameters exactly (in the absence of noise) as long as $t_{SOE} > t_r$, i.e., as long as $P_{mus}(t)$ returns 0 before the ventilator cycles off. Two different numerical algorithms are used to solve the quadratic programs at the core of the method, namely the active-set and interior-point algorithms (both available in Matlab® function `quadprog`). The former is more accurate when the true solution is found, the latter is faster (on

Table I. Deterministic example. Estimated R and E from data simulated with the following ventilator settings and patient parameters: $PEEP$=5, PSV=17, T_{rise}=0.3, R_v=2, R=7, E=20, $P_{mus}(t)$ from (11) with t_p=0.45, t_r=0.6, t_N=4. E_{cycle} is varied between 0.15 and 0.55 to generate breaths with positive and negative t_{SOE}-t_r. The parameters in the estimation algorithm are t_q=0.8, search for optimal t_m over [0,0.6] in increments of 0.05, R_{min}=E_{min}=0, R_{max}=E_{max}=100, $\tilde{P}_{min}$=-30, $\tilde{P}_{max}$=15.

E_{cycle}	t_{SOE}	t_{SOE}-t_r	Active Set algorithm		Interior Point algorithm	
			R_{est}	E_{est}	R_{est}	E_{est}
0.15	1.11	0.51	7.0000	20.0000	7.0000	20.0001
0.20	0.94	0.34	7.0000	20.0000	7.0001	20.0002
0.25	0.76	0.16	7.0000	20.0000	7.0008	20.0018
0.30	0.61	0.01	7.0000	20.0000	7.0008	20.0018
0.35	0.60	0.00	11.5180	30.0401	10.1807	27.0685
0.40	0.59	-0.01	6.7204	19.3786	10.3482	27.4409
0.45	0.58	-0.02	6.8956	19.7681	10.4334	27.6300
0.50	0.57	-0.03	6.7284	19.3964	10.4423	27.6498
0.55	0.56	-0.04	11.5180	30.0401	10.4193	27.5987

This article has been accepted for publication in a future issue of this journal, but has not been fully edited. Content may change prior to final publication. Citation information: DOI 10.1109/TBME.2015.2470641, IEEE Transactions on Biomedical Engineering

a laptop with 2.6 GHz Intel® Core™ i7 processor, the average computational time for a breath is 1 s for the interior-point algorithm vs. 5 s for the active-set algorithm). With the interior-point algorithm, the final error of the iterations causes errors in the estimates of R and E of less than 0.1%. Hence, the interior-point algorithm is preferred in the real-time application at hand and will be used in the rest of the paper.

As an example representative of the case $t_{SOE} > t_r$, Fig. 4a shows the simulated waveforms $P_{ao}(t)$, $\dot{V}(t)$ and $V(t)$ for $E_{cycle} = 0.2$ and Fig. 4b reports the corresponding output of the quadratic programs run for different values of t_m (in the search for the optimal t_m, expected to be $t_m = t_p$). Note how the estimates of R and E are very accurate in a relatively large range of t_m values. This means that the estimates are not very sensitive to the values of t_m chosen in the quadratic program. A full search for t_m is then not necessary for practical purposes and can be done over a reduced grid of values. Additionally, even though the presence of measurement noise might shift the position of the minimum of the cost function to a value $t_m \neq t_p$, the estimates of R and E are expected not to be significantly affected. In summary, the estimation method can be made computationally efficient and is expected to be robust to noise. In Fig. 4b, it is worth noting how for both R and E the estimate obtained via the method presented is significantly better than the one obtained via the ordinary LS method assuming the patient is passive (e.g. [5]). Also note how the value of t_q does not affect the method as long as $t_q \geq t_r$. In practice, since t_r is unknown, a possible approach consists of setting $t_q = t_{SOE}$ and limiting the search for t_m to the interval $t_1 \leq t_m < t_{SOE}$. t_{SOE} is provided by a standard ventilator, hence it is available to the estimation algorithm.

It is of interest to analyze what happens when $E_{cycle} \geq 0.35$, where Table I suggests that the estimation method is not able to find the exact solution. As a representative example, Fig. 5 shows more details for the case with $E_{cycle} = 0.4$. The comments are very similar to the case with $E_{cycle} = 0.2$, except for the fact that when $t_m = t_p$ the quadratic program does not yield the correct solution. As shown in Fig. 6, the interior-point algorithm converges to the minimum of the cost function (which, within the convergence tolerance, corresponds to perfect fitting, since no noise affects the data), as expected. However, the estimated R and E are not equal to the nominal values. In this specific example they actually are quite different. Understanding this event via eigenvalue decomposition gives a satisfactory explanation to this undesired result. Any solution consisting of R, E, $\tilde{P}_{mus}(t_1), \dots, \tilde{P}_{mus}(t_N)$ values can be written as a linear combination of the eigenvectors of H, the quadratic matrix of the cost function. As mentioned in the *Problem Statement* section, the analysis of the eigenvectors of H reveals two null eigenvalues. In the above-mentioned linear combination, the coefficients multiplying the eigenvectors corresponding to such null eigenvalues can be arbitrarily modified without affecting the value of the cost function. This gives rise to infinitely many solutions minimizing J in (7a). The introduction of the constraints in (7b)-(7d) aims to make these infinitely many solutions infeasible, except for the physiological solution corresponding to the respiratory resistance R and elastance E. Unfortunately, the eigendecomposition analysis reveals that when $t_{SOE} \leq t_r$ and the chosen t_m and t_q give rise to constraints perfectly compatible with the nominal $P_{mus}(t)$, such constraints are not sufficient to make the solution of the quadratic program in (7) unique. Fig. 7 shows the two eigenvectors corresponding to null eigenvalues for the H matrix arising in the case with $t_m = t_p$, circled in Fig. 5b. To be more precise, the plots in Fig. 7 refer only to the entries of such eigenvectors corresponding to $\tilde{P}_{mus}(t_1), \dots, \tilde{P}_{mus}(t_N)$. The entries corresponding to R and E are reported in the legend. Fig. 7 also shows that there exists a linear combination of such eigenvectors that is perfectly compatible with the constraints in (7b)-(7d) when the latter are chosen with $t_m = t_p = 0.45$ and $t_q = 0.8 \geq t_r = 0.6$. Such a linear combination of eigenvectors, multiplied by an arbitrary

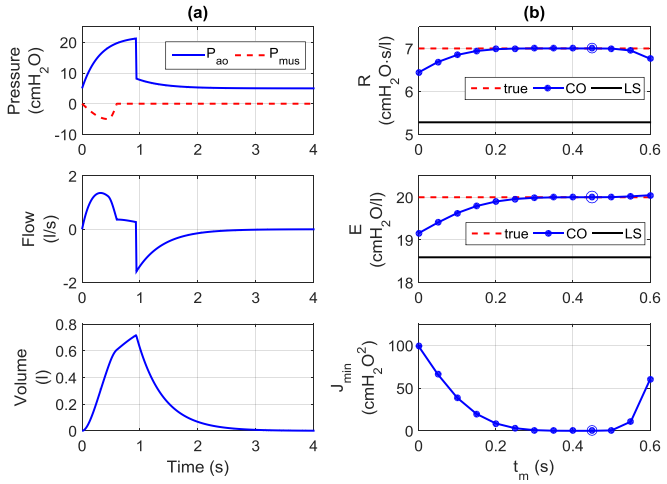

Fig. 4. Example with E_{cycle}=0.2 from Table I. (a) Simulated waveforms; (b) estimates of R and E and minimum cost function J_{min} from executions of the quadratic program in (7) for different values of t_m. The minimum among all J_{min}`s and the corresponding estimates are circled. Such values are the outcome of the presented estimation method.

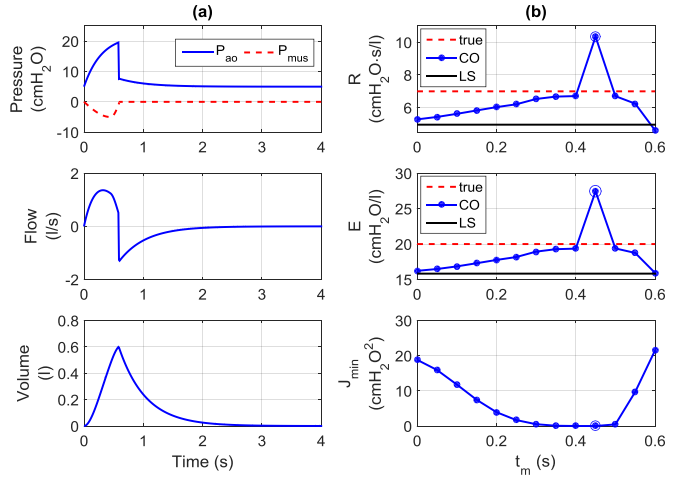

Fig. 5. Example with E_{cycle}=0.4 from Table I. (a) Simulated waveforms; (b) estimates of R and E and minimum cost function J_{min} from executions of the quadratic program in (7) for different values of t_m. The minimum among all J_{min}`s and the corresponding estimates are circled. Such values are the outcome of the presented estimation method.

This article has been accepted for publication in a future issue of this journal, but has not been fully edited. Content may change prior to final publication. Citation information: DOI 10.1109/TBME.2015.2470641, IEEE Transactions on Biomedical Engineering

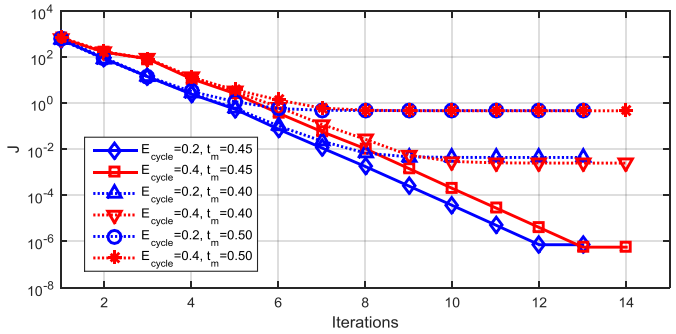

Fig. 6. Examples of convergence of the quadratic programs for the cases shown in Figs. 4 and 5. Convergence to the minimum J is always achieved, in both E_{cycle}=0.2 and E_{cycle}=0.4 cases. For $t_m = 0.45$, the minimized values of J are lower since the true P_{mus} reaches its minimum at $t_p = 0.45$. For other values of t_m, the constraints in (5) are not compatible with the true P_{mus}, therefore the minimum attainable J is higher.

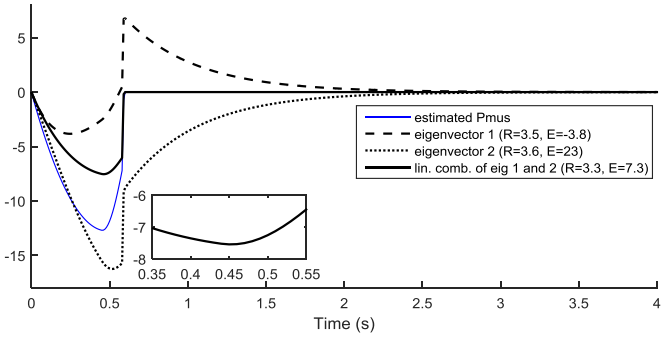

Fig. 7. Example with E_{cycle}=0.4, t_m=0.45 and t_q=1. There exists a linear combination of the two eigenvectors of H corresponding to zero eigenvalues that is compatible with the constraints. This illustrates how the solution to the quadratic program is not unique when $t_{SOE} \leq t_r$, $t_m = t_p$ and $t_q \geq t_r$. The linear combination of eigenvectors has its minimum value at t=0.45 (inset figure) and is constant for all t>1.

scaling factor, can be added to the solution that is found by the quadratic program, since it does not violate the constraints, without increasing the value of the cost function, because it is a linear combination of eigenvectors corresponding to zero eigenvalues (hence, the contribution to J is zero). This proves how the solution to the optimization problem is not unique when $t_{SOE} \leq t_r$ and the constraints are perfectly compatible with the true $P_{mus}(t)$. The iterative algorithm to solve the quadratic program then terminates once any feasible and minimizing solution is found. The solution we are after is one among several feasible and minimizing solutions. As shown in Table I, the desired solution is not guaranteed to be found. If the constraints are not compatible with the true $P_{mus}(t)$, for example because $t_m \neq t_p$, then the linear combination of eigenvectors shown in Fig. 7 cannot be added to the estimated $P_{mus}(t)$ found by the quadratic program because it would violate the constraints. Hence, for $t_m \neq t_p$ the quadratic program has a unique solution. Although this is not the desired solution, it gets closer to the true solution as t_m approaches t_p, as shown in Fig. 5b. Hence, for $t_{SOE} \leq t_r$, the case with t_m and t_q giving rise to constraints perfectly compatible with the nominal $P_{mus}(t)$ is a singular case. It is sufficient to solve a quadratic program with t_m slightly different from the nominal t_p to obtain estimates of R and E very close to the desired nominal values. We can state, therefore, that in the absence of noise, disturbances or modeling error, the estimate obtained from the method presented is exact in the limit of the constraints approaching compatibility with the nominal $P_{mus}(t)$. For constraints perfectly compatible with the nominal profile of $P_{mus}(t)$, the estimate is indeed exact if $t_{SOE} > t_r$, whereas it is generally not exact for $t_{SOE} \leq t_r$. For constraints *not* perfectly compatible with the nominal profile of $P_{mus}(t)$, the estimate is close to the desired nominal value.

One can then think of avoiding the problem due to the singularity by choosing an estimate from the neighborhood around the singularity, possibly making the constraints intentionally incompatible with the true profile of $P_{mus}(t)$. However, in practice the measurements are affected by noise and the optimization problem is generally ill-conditioned around the singularity. Hence, when $t_{SOE} \leq t_r$ there is no guarantee that the estimates of R and E are indeed close to the desired true values. The choice of $t_q = t_{SOE}$ (with $t_1 \leq t_m < t_{SOE}$) is an attempt to address the singularity of the method. Such a choice forces the algorithm to find a profile of $P_{mus}(t)$ that becomes constant right after t_{SOE}, making the constraints incompatible with the true profile of $P_{mus}(t)$ when $t_{SOE} \leq t_r$. Unfortunately, the effectiveness of this choice is difficult to generalize when $t_{SOE} \leq t_r$. If t_{SOE} occurs very close to t_r, the constraints might not be sufficiently incompatible with the true profile of $P_{mus}(t)$, resulting in high variance of the estimates (ill-conditioning). On the other hand, if t_{SOE} occurs very close to t_p, the constraints might introduce significant error from the true profile of $P_{mus}(t)$, resulting in high bias of the estimates. Conversely, as previously explained, the choice of $t_q = t_{SOE}$ does not affect the method capability of finding the desired solution when $t_{SOE} > t_r$.

B. Stochastic Example

The next example shows how the method performs in the presence of noise in the data. For the purpose, gaussian noise with zero mean and different values of standard deviation (0.1, 0.5, 1) is generated and added to $P_{ao}(t)$ to simulate noisy data in the model in (1). Additionally, it is of interest to see how the method responds to a nominal profile of $P_{mus}(t)$ that does not feature a well defined t_r. In real breaths, the respiratory muscles usually relax gradually and it is typical to assume an exponential decay of $P_{mus}(t)$ to 0. Like, for instance, in [24] and [25], the nominal $P_{mus}(t)$ is chosen to have the following parabolic-exponential profile

$$P_{mus}(t) = \begin{cases} \frac{P_p}{t_p(t_N - t_p)}(t_N t - t^2) & \text{for } 0 \leq t < t_p \\ P_p \frac{\exp\left(-\frac{(t-t_p)}{\tau_r}\right) - \exp\left(-\frac{(t_N - t_p)}{\tau_r}\right)}{1 - \exp\left(-\frac{(t_N - t_p)}{\tau_r}\right)} & \text{for } t_p \leq t < t_N \end{cases} \quad (12)$$

where τ_r is the time constant of the relaxation of the muscles. The decaying exponential approaches 0 asymptotically. Hence, $P_{mus}(t)$ never becomes exactly constant.

Table II reports the results of Monte Carlo simulations for the case with $E_{cycle} = 0.2$. The mean and standard deviation of the estimates obtained for R and E over 100 runs are shown and demonstrate how the bias introduced by noise is negligible

This article has been accepted for publication in a future issue of this journal, but has not been fully edited. Content may change prior to final publication. Citation information: DOI 10.1109/TBME.2015.2470641, IEEE Transactions on Biomedical Engineering

compared to the bias that one would have by neglecting $P_{mus}(t)$ and using the ordinary LS method (Figs. 4b and 5b).

V. Experimental Results

To verify the effectiveness of the presented technique in real case scenarios, the estimation method has been retrospectively tested on available experimental data. The data were collected as part of an educational study performed at the Pulmonary Research and Animal Laboratory at Duke University Medical Center on a 44 kg adult male pig. The experimental protocol was approved by the local institutional review board committee. During the study, a pig was anesthetized, intubated and connected to an Esprit ventilator with NM3 respiratory monitor (Philips-Respironics). Airway pressure (P_{ao}) and flow ($\dot{V}$) were measured at the Y-juncture, between the breathing circuit and the endotracheal tube, via the standard proximal sensors of the NM3 monitor. The pressure inside the esophagus (P_{es}) was measured as a surrogate of intrapleueral pressure (P_{pl}) using an esophageal balloon connected to a differential pressure transducer (Model PS309D, Validyne Engineering, Northridge, CA). Occlusion tests were performed to assess the correct positioning of the balloon as described in [13]. Data were acquired and collected at 100 Hz using a dedicated system for real-time data acquisition and computation.

The datasets used to test the algorithm are related to periods during which the pig was subject to continuous positive airways pressure (CPAP) with variable levels of pressure support ventilation (PSV). Two datasets were collected, for a total of 312 consecutive breaths. The performance of the algorithm presented was evaluated by comparing the resistance and elastance noninvasively estimated via the presented constrained optimization (CO) method (R_{CO} and E_{CO}) with their invasive counterparts (R_{inv} and E_{inv}). The invasive estimates are used as a gold standard and were obtained from the esophageal pressure data according to the following procedure:

(1) At the end of the study, the pig was placed on volume control ventilation (VCV) in order to be ventilated passively with moderate to high tidal volumes so that its spontaneous respiratory drive was temporarily inhibited ($P_{mus}(t) = 0$ in (1)). The flow ($\dot{V}$) and pressure (P_{ao} and P_{es}) data from five such passive breaths were then used to compute the resistance and elastance of the chest wall (R_{cw} and E_{cw}) via the LS algorithm. This method fits the data via the equation representing the part of the electrical analogue in Fig. 1b that pertains to the chest wall (i.e., from P_{pl} to P_{mus}), namely

$$P_{pl}(t) = R_{cw}\dot{V}(t) + E_{cw}V(t) + P_0''. \quad (13)$$

where P_0'' is, again, a constant pressure term to balance the equation at $t = 0$. The LS method yielded values of R_{cw} and E_{cw} for each selected passive breath. Final estimates of R_{cw} and E_{cw} were then obtained by averaging across five individual VCV breaths.

(2) The resistance and elastance of the airways/lungs (R_{aw} and E_L) were computed breath by breath across all the 312 breaths. The LS method was applied to fit (2) to the breath-by-breath flow ($\dot{V}$) and pressure (P_{ao} and P_{es}) data. Note that thanks to the use of P_{es} as a surrogate for P_{pl}, estimation of R_{aw} and E_L via LS is, in this case, a fully tractable mathematical problem since all the signals in (2) are known and the only unknowns are the parameters R_{aw} and E_L.

(3) Finally, the invasive respiratory system resistance and elastance estimates were computed by combining the chest wall and the lungs/airways parameters according to

$$R_{inv} = R_{cw} + R_{aw} \quad (14a)$$
$$E_{inv} = E_{cw} + E_L. \quad (14b)$$

The experimental results are summarized in Figs. 8–12. Fig. 8 shows the results from the first dataset. The top three plots show the experimental pressure and flow data, whereas the bottom two plots show the comparison between invasive and noninvasive estimates of resistance (R) and elastance (E). Two different noninvasive estimates are reported: those obtained via the presented CO method and those obtained via the ordinary LS method (e.g., [5]) assuming no patient effort is present ($P_{mus}(t) = 0$). The top plot also reports the fitting error from the presented estimation method (CO). The periods with missing data in the resistance and elastance plots correspond to periods that were excluded because the invasive and/or the noninvasive parameters could not be reliably computed due to artifacts in the experimental pressure and flow data. For instance, artifacts in the esophageal pressure waveform around 1100 s are most likely due to esophageal spasms (and hence not real diaphragmatic activity). These were thus excluded from the computation of the invasive estimates. Similarly, artifacts in the pressure and flow data (around 400 and 1000 s), due to auto-calibration of the sensors operated by the NM3 software, precluded the computation of both the invasive as well as the noninvasive estimates. As we can notice from the P_{ao} waveform (top plot of Fig. 8), the dataset includes periods at different PSV levels. Particularly, after 100 s at 5 cmH_2O, PSV is progressively reduced throughout the dataset from 20 to 10 cmH_2O in steps of 3 cmH_2O at intervals of 5 minutes, as indicated by a reduction in the peak airway pressure values. This is associated with a drop in peak flow (see middle plot of Fig. 8). The reduction in peak

Table II. Stochastic example. Estimated R and E (mean and standard deviation over Monte Carlo Simulations with 100 runs). The data are simulated with the following ventilator settings and patient parameters: $PEEP$=5, PSV=17, T_{rise}=0.3, E_{cycle}=0.2 R_v=2, R=7, E=20, $P_{mus}(t)$ from (12) with P_p=-5, t_p=0.5, τ_r=0.05, t_N=4. The parameters in the estimation algorithm are t_q=t_{SOE}, search for optimal t_m over $[0, t_{SOE})$ in increments of 0.05, R_{min}=E_{min}=0, R_{max}=E_{max}=100, $\tilde{P}_{min}$=-30, $\tilde{P}_{max}$=15. Three Monte Carlo simulations are shown, each with different noise standard deviation (0.1, 0.5, 1).

Noise	Resistance			Elastance		
	True	Estimate		True	Estimate	
Std dev		Mean	Std dev		Mean	Std dev
0.1	7	7.023	0.023	20	20.047	0.042
0.5	7	7.153	0.126	20	20.312	0.235
1	7	7.353	0.262	20	20.712	0.498

This article has been accepted for publication in a future issue of this journal, but has not been fully edited. Content may change prior to final publication. Citation information: DOI 10.1109/TBME.2015.2470641, IEEE Transactions on Biomedical Engineering

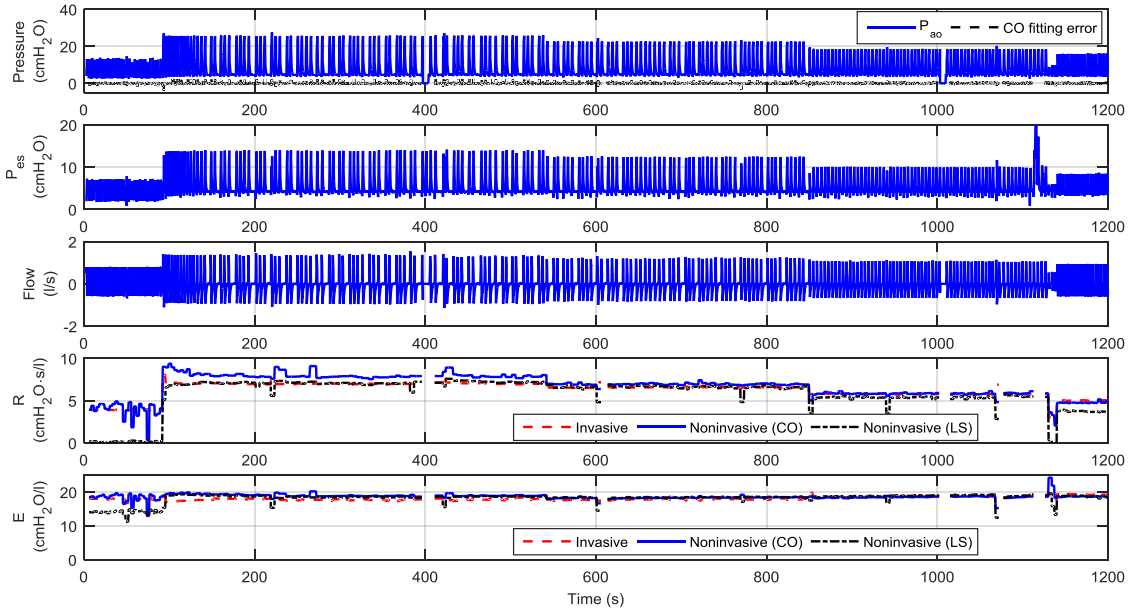

Fig. 8. Comparison between invasive and noninvasive estimates on the first experimental dataset. From top to bottom: measured airway pressure (P_{ao}) and CO fitting error, esophageal pressure (P_{es}), flow, estimated resistance (R) and elastance (E). The inputs to the CO estimation method are, for every breath, the waveforms of airway pressure, flow and volume as well as the ventilator t_{SOE} (from NM3 respiratory monitor). The parameters in the CO estimation method are t_q=t_{SOE}, search for optimal t_m over [0, t_{SOE}) in increments of 0.05, R_{min}=E_{min}=0, R_{max}=E_{max}=100, $\tilde{P}_{min}$=-30, $\tilde{P}_{max}$=15. The quadratic programs are solved by the interior-point algorihtm (Matlab® function `quadprog`). The esophageal pressure measurements are not used by the CO nor LS estimation methods. They are used to compute the invasive estimates.

flow correlates with a reduction in R_{inv}. This is due to the dependence of the resistance on the flow, as reported in the literature (e.g., Rohrer's equation [26]). Conversely, the elastance E_{inv} appears to be unaffected by the variations in respiratory patterns throughout the dataset. From Fig. 8, we can observe that the agreement between invasive and (noninvasive) CO estimates is remarkable, across PSV changes. A bias of about 1 cmH_2O·s/l in the CO estimates of R can be noticed from 100 to 500 s (PSV of 20). The analysis of the P_{mus} waveforms that can be reconstructed from the measured P_{es} data and the estimated chest wall parameters R_{cw} and E_{cw} (Fig. 9) suggests that, during this period, the pig was "fighting" the ventilator (i.e., exerting positive P_{mus} during inhalation). For lower PSV values, minimum or no positive effort was made by the pig. The presence of a positive P_{mus} deflection violates the assumptions behind the constraints in (5) at the core of the CO estimation method. A significant positive deflection (amplitude of the anomalous positive deflection comparable to the amplitude of the negative deflection indicating inspiratory effort) like at PSV of 20 gives then rise to bias in the estimates from CO and overall poorer fitting of (1). As the positive deflections become smaller at lower PSV, the bias tends to disappear.

Fig. 10 shows the results from the second dataset. In this case, the PSV level was gradually increased from 5 to 15 cmH_2O in steps of 5 cmH_2O. Again, the changes in PSV correlate with changes in R_{inv}. Similar to the results from the first dataset, the periods with missing data in the resistance and elastance plots are due to artifacts in the esophageal pressure data that prevented the computation of reliable R_{inv} and E_{inv} estimates. Even in this case, the agreement between the invasive and (noninvasive) CO estimates of resistance and elastance is satisfactory, except for a few breaths at the lowest PSV for which the CO algorithm underestimates both R and E. Fig. 11 shows a zoom in on such cases. A deeper analysis of the P_{ao} waveform reveals, in the incorrectly estimated breaths, the absence of the positive spikes that characterize all the other correctly estimated breaths (dashed ellipses in Fig. 11). The positive spikes in P_{ao} right before the ventilator cycles off can be interpreted as a sign of rapid decrease of inspiratory activity. A reduction in P_{mus} acts as a disturbance for the ventilator controller that regulates P_{ao}. Since the controller is not ideal, it requires some time to respond to this disturbance. As a consequence, the reduction in P_{mus} gets reflected as a temporary increase in P_{ao}. These findings are in agreement with the limitations of the estimation algorithm highlighted in the *Numerical Validation* section. When the decrease in P_{mus} occurs *before* the ventilator cycles off (spike in P_{ao}), the algorithm yields accurate estimates. Conversely, the CO estimates that are far from the invasive ones emanate from breaths for which the ventilator cycles off before the decrease in P_{mus} occurs. Such breaths are more frequent in regions of low PSV, where P_{mus} is generally more sustained and likely to extend past the ventilator cycling off. The same phenomenon occurs in the first 100 s of the first dataset.

Finally, Fig. 12 summarizes the overall performance of the presented method on all 312 breaths. Fig. 12a shows the linear regression plots, where the noninvasive CO estimates are plotted against the corresponding invasive estimates. The red lines represent the diagonals along which the data would lie if perfect agreement existed. Fig. 12b shows the Bland-Altman plots, where the absolute errors (noninvasive minus invasive estimates) are plotted as function of the invasive estimates. The black dashed lines indicate the accuracy of the presented

This article has been accepted for publication in a future issue of this journal, but has not been fully edited. Content may change prior to final publication. Citation information: DOI 10.1109/TBME.2015.2470641, IEEE Transactions on Biomedical Engineering

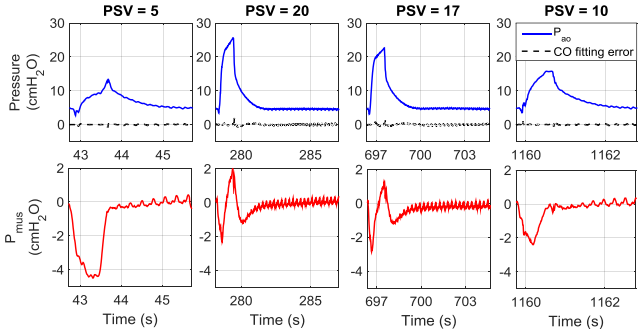

Fig. 9. Snapshots of breaths from different segments of the dataset in Fig. 8. Top plots: measured airway pressure (P_{ao}) and CO fitting error. Bottom plots: respiratory muscle pressure (P_{mus}) reconstructed from measured esophageal pressure (P_{es}) and estimated chest wall parameters (R_{cw} and E_{cw}).

estimation method computed as the mean of the absolute errors. The red dashed lines indicate the precision of the presented method computed as ± 1 standard deviation of the absolute error. The method provides resistance estimates with a bias of 0.27 and precision of 0.79. These correspond to 4.5% and 13.1% of the mean value of R_{inv} over the entire dataset, respectively. The elastance, on the other hand, is estimated with a bias of 0.37 and precision of 1.20, corresponding to 2.0% and 6.4% of the mean E_{inv}, respectively. It is envisioned that these small biases and errors would be generally acceptable to the clinical community. Note that these statistics include all the breaths shown in Figs. 8 and 10, i.e., also the breaths with anomalous response of the pig at PSV of 20 in the first dataset as well as the breaths with early ventilator cycling off in both datasets. As a last note, the average computational time per breath over the two experimental datasets was 1.6 s on a laptop with 2.6 GHz Intel® Core™ i7 processor, which is suitable for the intended real-time application.

VI. Discussion

Continuous, noninvasive measurements of lung function has been long desired, especially in the intensive care unit (ICU) for patients in respiratory failure and requiring mechanical ventilation. The method presented in this paper takes in pressure and flow at the mouth (or Y-juncture for patients ventilated with an endotracheal tube) and outputs the patient respiratory resistance and elastance. These quantities help the clinician understand basic mechanical properties of the respiratory system and thus make decisions about providing (and withdrawing) mechanical respiratory support.

The main characteristics of the presented method can be summarized as follows: i) The estimation technique is noninvasive (airway pressure and flow are available for any ventilated patient); ii) The algorithm processes data from an entire breath to output patient respiratory elastance and resistance; iii) The method is designed to take into account respiratory effort from the patient, hence it is suitable for spontaneously breathing patients as is the case in PSV mode; iv) It is based on a mechanistic model of respiratory physiology; v) It overcomes the underdetermined nature of noninvasive estimation of respiratory mechanics by adding physiological constraints to the unknowns to be estimated.

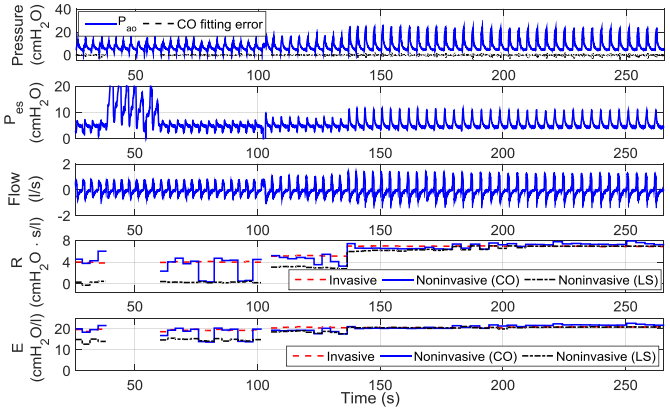

Fig. 10. Comparison between invasive and noninvasive estimates on the second experimental dataset. From top to bottom: measured airway pressure (P_{ao}) and CO fitting error, esophageal pressure (P_{es}), flow, estimated resistance (R) and elastance (E). The inputs and parameters of the CO estimation methods are the same as for the first experimental dataset (Fig. 8).

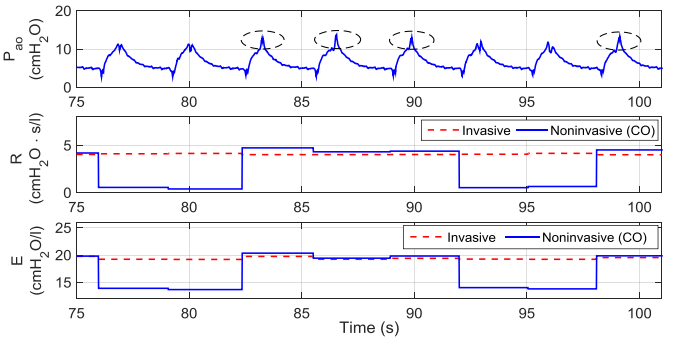

Fig. 11. Zoom in on Fig. 10 around four of the incorrectly estimated breaths from the second experimental dataset. From top to bottom: airway pressure (P_{ao}), resistance (R) and elastance (E).

These constraints are general and only assume passive exhalation (no positive P_{mus} during exhalation) and no patient double effort during inhalation (no double negative peak in P_{mus} during inhalation). The occasional violation of these assumptions acts like a disturbance to the estimation method, as shown in the first experimental dataset (Figs. 8 and 9). Additionally, in contrast with the classic two-point method (see for instance [27]), the presented technique does not rely on zero-flow points to estimate the respiratory elastance. This is particularly important for patients affected by COPD (chronic obstructive pulmonary disease), whose typical dynamic hyperinflation makes the two-point method invalid as noted by Rossi *et al.* [28].

The numerical examples and their detailed analysis provide good insight into the general estimation problem and the presented method in particular. For instance, the examples show the importance of the inhalation breath segment where the ventilator is exciting the system (before cycling off) and the patient effort has already terminated ($P_{mus} = 0$ or, more rigorously, $P_{mus} = \text{constant}$). With a simpler approach, one could then think of the ordinary LS method applied only to data points for which P_{mus} can be considered to equal 0. The drawback is that – in practice – it is difficult to identify the time sample after which $P_{mus} = 0$. In the numerical examples such a time sample can be identified via the characteristic change in the slope of the flow, but with real waveforms the

This article has been accepted for publication in a future issue of this journal, but has not been fully edited. Content may change prior to final publication. Citation information: DOI 10.1109/TBME.2015.2470641, IEEE Transactions on Biomedical Engineering

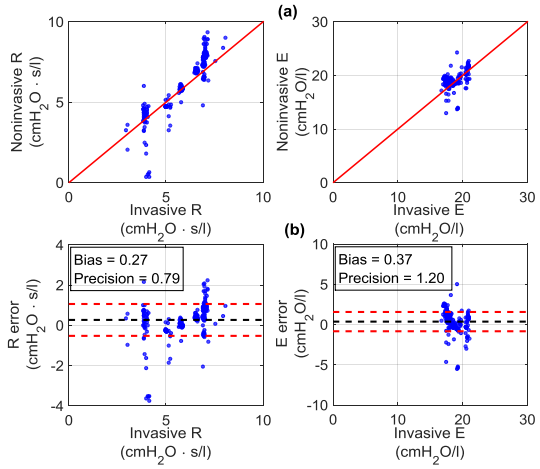

Fig. 12. Linear regression plots (a) and Bland-Altman plots (b) on the 312 breaths from two experimental datasets.

slope change is typically blurred if at all identifiable. In contrast, the presented method is a practical solution that only uses the SOE time sample, which is readily available from the ventilator, to automatically define constraints on $\tilde{P}_{mus}$. Furthermore, one may want to rely on the SOE time sample provided by the ventilator to apply the ordinary LS method to data for exhalation only (for which the assumption $P_{mus} = 0$ generally holds), fitting the model in (10a) or Fig. 3 instead of the model in (1) or Fig. 1c. However, that could, at best, yield the ratio of $R + R_v$ to E (i.e., the time constant of the system in Fig. 3), and not the actual values of the patient parameters R and E like the method presented in this paper. Additional complications in fitting (10a) arise with ventilators whose expiratory valve is controlled to intentionally change R_v during the exhalation phase. In contrast, the method presented in this paper is completely based on fitting (1). Hence, it does not suffer from time-varying R_v.

Both the numerical and experimental data validated the estimation method when the ventilator cycles off after the patient effort is over, which is the most frequent situation in mechanical ventilation practice. Also, the examples presented show how performance can degrade when the ventilator cycles off early, i.e., before P_{mus} vanishes. The mathematical justification for the estimation to become critical in such a condition was investigated and led to proposing a practical solution based on the SOE time sample that is already provided by the ventilator. However, its effectiveness cannot be generalized since it depends on the relative position between the SOE time sample and the times at which P_{mus} reaches its minimum value and returns to 0, which varies on a per case basis. The first experimental dataset also showed the presented method in action in conditions where its underlying assumptions are violated (positive P_{mus}). Additionally, both experimental datasets highlighted how the advantage of using the presented approach over the ordinary LS method is more significant as the respiratory muscle activity increases.

Although the estimation method has been demonstrated and validated in the most common ventilator support situations, further work will aim to improve its performance in the case of delayed ventilator cycling off. This could be achieved directly, for instance, by a different formulation of the constraints in the optimization problem. Alternatively, similar to the automated respiratory cycles selection approach proposed by Rigo *et al*. [29], the presented method could be complemented with indicators of anomalous conditions of ventilation that are detrimental for the estimation algorithm. Taking into account the strengths and weaknesses of the presented estimation technique, we envision that the method could be utilized in conjunction with algorithms that would detect either asynchrony in the cycling off of the ventilator, or activity of the expiratory muscles, or patient double effort during inhalation. These algorithms would detect such anomalous conditions without the additional challenge of their quantification. Their output would suggest whether the estimates from the presented constrained optimization approach are reliable. Since such anomalous conditions are usually clinically undesirable, the clinician would, typically and based on experience or on the alerts generated by the envisioned detection algorithms, adjust the ventilator settings so that the ventilation conditions return to normal. In turn, normal ventilation conditions are the most favorable for the presented estimation method.

One of the limitations of this study is that only data from healthy animals and numerical simulations were used. Further studies on patients with broader variation of respiratory mechanics parameters are anticipated to better assess the efficacy of the presented technique in real clinical settings.

VII. Conclusion

The paper presented a method for the estimation of respiratory resistance and elastance in spontaneously breathing mechanically ventilated patients. Compared to existing techniques, the new method is noninvasive, does not require maneuvers interfering with the desired ventilation patterns and takes into account the possibility of respiratory muscles effort, making the technique suitable even for spontaneously breathing patients. The method is based on a mechanistic mathematical model of the lung mechanics, more specifically on a single-compartment first-order linear model widely accepted in the respiratory research community. At the core of the method is the minimization of an objective function subject to physiological constraints that aim to overcome the underdetermined nature of the estimation problem in the presence of patient effort. Both numerical simulations and animal data are used to illustrate and validate the method. Assumptions, strengths and weaknesses are also discussed.

The method makes it possible to continually estimate respiratory elastance and resistance in both passive and active patients during normal operation of the ventilator. Continual noninvasive insight into respiratory mechanics holds the promise that clinicians will be able to better provide mechanical ventilator support with fewer adverse effects and ultimately better outcomes.

This article has been accepted for publication in a future issue of this journal, but has not been fully edited. Content may change prior to final publication. Citation information: DOI 10.1109/TBME.2015.2470641, IEEE Transactions on Biomedical Engineering

REFERENCES

[1] D. C. Grinnan and J. D. Truwit, "Clinical review: respiratory mechanics in spontaneous and assisted ventilation,"*Crit. Care*, vol. 9, no. 5, pp. 472–484, 2005.

[2] G. Polese *et al.*, "Respiratory mechanics in the intensive care unit," *Eur. Respir. Monogr.*, vol. 31, pp. 195–206, 2005.

[3] G. Nucci and C. Cobelli, "Mathematical models of respiratory mechanics," in *Modeling methodology for physiology and medicine*, 1st ed., San Diego, CA: Academic Press, 2001, ch. X, pp. 279–304.

[4] R. Peslin *et al.*, "Respiratory mechanics studied by multiple linear regression in unsedated ventilated patients," *Eur. Respir. J.*, vol. 5, pp. 871–878, 1992.

[5] G. A. Iotti *et al.*, "Respiratory mechanics by least squares fitting in mechanically ventilated patients: application during paralysis and during pressure support ventilation," *Intensive Care Med.*, vol. 21, pp. 406–413, 1995.

[6] J. H. Bates, "The Linear Single-Compartment Model," in *Lung Mechanics - an Inverse Modeling Approach*, Cambridge, UK: Cambridge University Press, 2009, pp. 47–49.

[7] A. G. Polak, "Analysis of multiple linear regression algorithms used for respiratory mechanics monitoring during artificial ventilation," *Comput. Methods Programs Biomed.*, vol. 101, pp. 126–134, 2011.

[8] L. Ljung and T. Soderstrom, *Theory and practice of recursive identification*. Cambridge, MA: MIT Press, 1983.

[9] A. M. Lauzon and J. H. Bates, "Estimation of time-varying respiratory mechanical parameters by recursive least squares," *J. Appl. Physiol.*, vol. 71, pp. 1159–1165, 1991.

[10] J. H. Bates and A. M. Lauzon, "A nonstatiscal approach to estimating confidence intervals about model parameters: application to respiratory mechanics," *IEEE Trans. Biomed. Eng.*, vol. 39, pp. 94-100, 1992.

[11] G. Avanzolini *et al.*, "A new approach for tracking respiratory mechanical parameters in real-time," *Ann. Biomed. Eng.*, vol. 25, pp. 154–163, 1997.

[12] S. Khirani *et al.*, "On-line monitoring of lung mechanics during spontaneous breathing: a physiological study," *Respir. Med.*, vol. 104, pp. 463-471, 2010.

[13] J. O. Benditt, "Esophageal and gastric pressure measurements," *Respir. Care*, vol. 50, no. 1, pp. 68–75, 2005.

[14] R. Kuhlen and C. Putensen, "Maintaining spontaneous breathing efforts during mechanical ventilatory support," *Intensive Care Med.*, vol. 25, pp. 1203–1205, 1999.

[15] C. Putensen *et al.*, "Long-term effects of spontaneous breathing during ventilator support in patients with acute lung injury," *Am. J. Respir. Crit. Care Med.*, vol. 164, pp. 43–49, 2001.

[16] V. M. Kogler, "Advantage of spontaneous breathing in patients with respiratory failure," *SIGNA VITAE*, vol. 4, 2009.

[17] M. Younes *et al.*, "A method for measuring passive elastance during proportional assist ventilation," *Am. J. Respir. Crit. Care Med.*, vol. 164, pp. 50-60, 2001.

[18] M. Younes *et al.*, "A method for noninvasive determination of inspiratory resistance during proportional assist ventilation," *Am. J. Respir. Crit. Care Med.*, vol. 163, pp. 829-839, 2001.

[19] K. Lopez-Navas *et al.*, "Non-invasive determination of respiratory effort in spontaneous breathing and support ventilation: a validation study with healthy volunteers," *Biomed Tech.*, vol. 59, pp. 335–341, 2014.

[20] Y. Chiew *et al.*, "Time-varying respiratory system elastance: a physiological model for patients who are spontaneously breathing," *PLoS One*, vol. 10, 2015.

[21] B. Diong *et al.*, "The augmented RIC model of the human respiratory system," *Med. Biol. Eng. Comput.*, vol. 47, pp. 395–404, 2009.

[22] E. Oostveen *et al.*, "The forced oscillation technique in clinical practice: methodology, recommendations and future developments," *Eur. Respir. J.*, vol. 22, pp. 1026–1041, 2003.

[23] S. Boyd and L. Vandenberghe, *Convex Optimization*. Cambridge, UK: Cambridge University Press, 2004.

[24] Y. Yamada and H.-L. Du, "Analysis of the mechanisms of expiratory asynchrony in pressure support ventilation: a mathematical approach," *J. Appl. Physiol.*, vol. 88, pp. 2143–2150, 2000.

[25] A. Albanese *et al.*, "An integrated mathematical model of the human cardiopulmonary system: model development," *Am. J. Physiol.* (submitted for publication).

[26] F. Rohrer, "Flow resistance in human air passages and the effect of irregular branching of the bronchial system on the respiratory process in various regions of the lungs," *Arch. Ges. Physiol.*, vol. 162, pp. 225–299, 1915.

[27] Z. Zhao *et al.*, "Assessment of a volume-dependent dynamic respiratory system compliance in ALI/ARDS by pooling breathing cycles," *Physiol. Meas.*, vol. 33, pp. 61–67, 2012.

[28] A. Rossi *et al.*, "Measurement of static compliance of the total respiratory system in patients with acute respiratory failure during mechanical ventilation. The effect of intrinsic positive end-expiratory pressure," *Am. Rev. Respir. Dis.*, vol. 131, no. 5, pp. 672–677, 1985.

[29] V. Rigo *et al.*, "Automated respiratory cycles selection is highly specific and improves respiratory mechanics analysis," *Pediatr. Crit. Care Med.*, vol. 13, no. 4, pp. 234–239, 2012.

Francesco Vicario received the BS and MS degrees in mechanical engineering from Politecnico di Torino, Italy, in 2004 and 2006, the MS degree in operations research and the PhD degree in mechanical engineering from Columbia University, NY, in 2012 and 2014. Since 2015 he has been a research scientist at Philips Research North America. His main area of research is system identification, with applications in biomedical, aerospace and civil engineering.

Antonio Albanese received the BS and MS degrees in biomedical engineering from University of Bologna, Italy, in 2005 and 2008, and the PhD degree in biomedical engineering from Columbia University, NY, in 2014. Since 2013 he has been a research scientist at Philips Research North America. His main areas of research are mathematical modeling, parameter estimation and control of physiological systems.

Nikolaos Karamolegkos received the MS degree in electrical and computer engineering from University of Patras, Greece, in 2009 and the MS degree in biomedical engineering from Columbia University, NY, in 2012. In the same year, he received a fellowship from Philips Research NA to pursue the PhD degree in biomedical engineering. His research is focused on system identification and parameter estimation of physiological systems with application in medical devices.

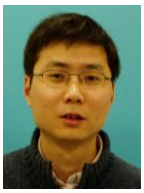

Dong Wang received the BS and MS degrees from Zhejiang University, Hangzhou, China, in 1996 and 1999, and the PhD degree from University of Delaware, DE, in 2005, all in electrical engineering. Since 2002 he has been with Philips Research, first in East Asia and then in North America, where he is currently a senior research scientist. His research interests include signal processing and data analytics for wireless communications and healthcare applications.

Adam Seiver serves as Chief Medical Affairs for Therapeutic Care, Philips Healthcare. His research focuses on decision support for critical care. After 20 years practice as a trauma surgeon, he now directs critical care telemedicine for Sutter Health in Sacramento, California. Dr. Seiver holds an MD and a PhD from Stanford, and an MBA from Duke. He is Board Certified in Surgery, Surgical Critical Care, and Clinical Informatics.

Nicolas W. Chbat is Principal Researcher at Philips Research North America, where he heads advanced engineering applications to critical care medicine. He is Adjunct Professor of biomedical and mechanical engineering at Columbia University. Previously, he worked at General Electric Global Research Center and Mayo Clinic. His research area is dynamic modeling, estimation, and controls. He holds a PhD from Columbia and is the 2013 IEEE EMBS Technical Achievement Award recipient.